Vol. 15, No. 1 (2026): 301 - 312 http://dx.doi.org/10.23960/jtepl.v15i1.301-312

JURNAL TEKNIK PERTANIAN LAMPUNG

ISSN 2302-559X (print) / 2549-0818 (online)

Journal homepage : https://jurnal.fp.unila.ac.id/index.php/JTP

The Impacts of Magnetic Fields on Combustion Characteristics of Virgin Coconut Oil Droplets

Wigo Ardi Winarko[1,✉], Yuke Hary Laksono[1]

[1] Heavy Equipment Engineering Department, Indonesian Heavy Equipment Engineering Academy, Malang, INDONESIA.

Article History:

Received : 25 September 2025
Revised : 17 October 2025
Accepted : 29 October 2025

Keywords:

Droplet Combustion,
Flame Stability,
Magnetic field,
Paramagnetic Force,
VCO.

Corresponding Author:
✉ wigo@akabi.ac.id
(Wigo Winarko)

ABSTRACT

Improving the combustion efficiency and stability of biofuels such as virgin coconut oil (VCO) is a major challenge in renewable energy development. This study aims to investigate quantitatively the effect of external magnetic field configuration on the freezing dynamics of single VCO droplets. The experiment was performed using combustion of a single droplet placed on a thermocouple that also functions as a temperature meter. To generate a flame, the droplet was heated using a heating element until it ignites. The VCO droplets were burnt under five conditions: without a magnetic field (WOM), and between two permanent magnets with four different pole configurations, attractive (N-S, S-N) and repulsive (N-N, S-S). The observation included flame morphology, temperature profile, flame height, burning rate, and ignition delay time. Results showed that the magnetic field significantly improves combustion performance. The flicker instability due to buoyancy can be eliminated, while the peak temperature increases from 761 °C in the WOM condition to 858 °C in the S-N configuration. Furthermore, the combustion rate increased, and the ignition delay time decreased from 4.99 s (WOM) to 3.43 s (N-S/S-N). Consistently, the attractive field configuration (N-S/S-N) yielded the best performance. These findings confirm that the magnetic field orientation serves as a key parameter to control the dynamics and enhance the combustion intensity of biofuels.

1. INTRODUCTION

The global energy crisis and increasing climate change, primarily driven by the widespread use of fossil fuels, have become challenges in science and technology. The use of petroleum and coal, which continues to increase every year, is the main cause of high air pollution, carbon dioxide (CO_2) emissions, nitrogen oxides (NO_x), and fine particles that have a negative impact on human health and global climate change (IEA, 2024; Wang *et al*., 2007). To prevent greater impacts, alternative renewable energy sources are needed that are environmentally friendly, locally available and clean pollution (Perdana *et al*., 2018). Among several alternative energy sources being developed by several scientific disciplines, biofuels or vegetable fuels are an alternative energy to reduce dependence on fossil fuels while reducing greenhouse gas emissions (Leung *et al*., 2010; Singh & Singh 2010). However, not all vegetable oils are suitable for use as fuel due to production limitations and less than optimal combustion properties.

Virgin Coconut Oil (VCO) is a biofuel with several advantages when viewed from the perspective of availability, physical and chemical properties of its components (Winarko *et al*., 2022). Based on data published by the FAO (Food and Agriculture Organization of the United Nations), Indonesia is the world's largest coconut producer with a total production of 17 million tons per year (Statista, 2025). This amount is very feasible if some of it is used for biofuel needs. Based on its fatty acid composition, VCO is largely dominated by saturated fatty acids, which provide a high flash point and oxidation stability (Ferreira de Souza *et al*., 2020). VCO is also dominated by lauric fatty acid, which significantly contributes to the stability and combustion efficiency of vegetable oils, making it suitable for application as a fuel (Ma & Hanna 1999; Srivastava & Prasad, 2000). Furthermore, the use of VCO as an alternative fuel also needs to be reviewed based on its physical properties. These physical properties significantly influence the flow characteristics, atomization, and evaporation of droplets during combustion (Pham *et al*., 2020). This includes viscosity and thermal stability, which influence combustion behavior. High viscosity tends to slow fuel atomization, which can impact combustion rate and flame efficiency (Moser, 2009; Parveg & Ratner, 2025). Therefore, a thorough understanding of VCO combustion characteristics is crucial for optimizing combustion performance and reducing emissions during combustion (Abdul Malik *et al*., 2017; Sharma *et al*., 2021).

Droplet combustion is a method that can be used to determine the combustion characteristics of a fuel, both in terms of its physical and chemical properties (Hoxie *et al*., 2014). Key parameters such as flame stability, flame temperature, combustion rate, and ignition delay time, which determine the combustion quality of VCO, can also be observed using the droplet combustion method (Zhu *et al*., 2020). This is because these parameters are related to the energy produced during combustion (Perdana *et al*., 2020). Ibadurrohman *et al*., (2022) stated that the length of the ignition delay time of a vegetable oil is influenced by the length of the carbon chain and its saturation level. This is because differences in carbon chains will result in different molecular reactivities when vegetable oil is exposed to high temperatures (Marlina *et al*., 2020). However, this process is also highly dependent on physical factors such as droplet size and fuel evaporation rate, which are influenced by the fuel's viscosity, surface tension, and thermal conductivity (San José Alonso *et al*., 2012). Therefore, understanding the chemical and physical properties of VCO is crucial for developing efficient and environmentally friendly biofuels.

In addition to internal fuel factors, external influences, such as magnetic fields, on the combustion process have begun to be widely studied. Several studies have shown that magnetic fields can alter the trajectories of electrons and free radicals during combustion, thus affecting chemical reactions and flame behavior (Hu *et al*., 2022; Pliss & Soloviev, 2022). By altering the chemical reactions in the fuel, the magnetic field effect is expected to influence the length of the ignition delay and increase flame stability (Agarwal *et al*., 2015; Jocher *et al*., 2017). Furthermore, magnetic fields modify oxygen supply, reducing flicker frequency, and altering flame height and length (Xie *et al*., 2021). The addition of a 5000 gauss magnetic field to a counter-flow burner can also increase flame area and stability, as well as increase temperatures in premixed and diffusion flames (Khlaif *et al*., 2023). The addition of a 4,000–8,000G neodymium magnetic field to a single-cylinder engine has been shown to significantly reduce HC and NO (Pramodkumar *et al*., 2017). The addition of a magnetic field to the fuel line can also reduce NO_x by up to 37% (Kurji & Imran, 2018). However, most of this research has focused on fossil fuels and natural gas. To date, the influence of magnetic fields on the combustion characteristics of liquid biofuels such as VCO, particularly at the droplet scale, is still very limited and has not been systematically studied (El-Fakharany *et al*., 2025; Kurji & Imran 2018; Sidheshware *et al*., 2023).

Based on this gap, and based on the importance of fundamental understanding through the droplet combustion method and the potential of magnetic fields in optimizing the combustion process, this study was conducted to evaluate the effect of magnetic fields on the combustion characteristics of VCO droplets through flame visualization analysis, flame temperature, combustion rate, flame height, and ignition delay time. This study is expected to be a new scientific contribution because it is one of the first studies to integrate the physical and chemical aspects of VCO combustion with the influence of magnetic fields. The results of the study are expected to not only enrich fundamental knowledge in biofuel combustion technology but also open up opportunities for innovation in the use of magnetic fields to increase efficiency while reducing emissions from biofuel combustion.

2. MATERIALS AND METHODS

The virgin coconut oil (VCO) used as fuel in this study was obtained from the extraction of coconut fruit and used directly as fuel without undergoing transesterification or other chemical purification processes. To maintain the chemical stability and purity of the VCO, the coconut fruit extraction process was carried out using a cold pressing method. Analysis of physical and chemical properties including kinematic viscosity, density, flash point, pour point, and fatty acid composition used as supporting data to analyze combustion characteristics can be seen in Table 1 and Table 2.

Table 1. Physical properties of virgin coconut oil

Properties	Unit	Method ASTM	VCO*
Density at 15 °C (kg/l)	Kg/l	D1298	925.7
Viscosity Kinematics at 40 °C	cSt	D445	25.82
Viscosity Kinematics at 100 °C	cSt	D445	5.664
Flash point	°C	D93	309.5
Pour point	°C	D97	21

*Source: (Dedison & Ismet, 2022)

Table 2. Fatty acid composition of virgin coconut oil

Properties	Unit	Method ASTM	VCO*
Saturated acid	Caprylic acid	$C_8H_{16}O_2$	7.4
	Capric acid	$C_{10}H_{20}O_2$	6.3
	Lauric acid	$C_{12}H_{24}O_2$	48.1
	Myristic acid	$C_{14}H_{28}O_2$	18.7
	Palmitic acid	$C_{16}H_{32}O_2$	9.1
	Stearic acid	$C_{18}H_{36}O_2$	2.6
	Arachidic acid	$C_{20}H_{40}O_2$	–
Unsaturated acid	Oleic acid	$C_{18}H_{34}O_2$	6.4
	Linoleic acid	$C_{18}H_{32}O_2$	1.4
	Linolenic acid	$C_{18}H_{30}O_2$	–
	Eicosanoic acid	$C_{20}H_{40}O_2$	–
Saturated acid			92.2
Monounsaturated acid			6.4
Polyunsaturated acid with two or more double bonds			1.4

To study the characteristics of micro combustion, a single droplet combustion system was used which was assumed to be similar to the misting of a diesel engine nozzle. In the test, VCO droplets with a diameter of 0.79 – 0.82 mm were formed precisely using a micro pipette with a setting of 1.5 ul (4), then the droplets were placed at the connection point between two 0.1 mm diameter k-type thermocouple wires (5). To ensure the diameter remained the same, the diameter of each data produced was also measured using the Image J software. In addition to functioning as a support for the droplets so they do not fall, the thermocouple also functions to read the flame temperature during the test. The initial heating process during the test was carried out with the help of a nichrome heating element which was placed directional under the droplet (3). As the main variable of the study, a magnetic field was applied to the combustion area. Two permanent magnet bars were placed on the left and right sides of the droplet (1). The magnets were placed on a holder to maintain a constant condition even though the field orientation changed (2). Details of the position of each component can be seen in Figure 1.

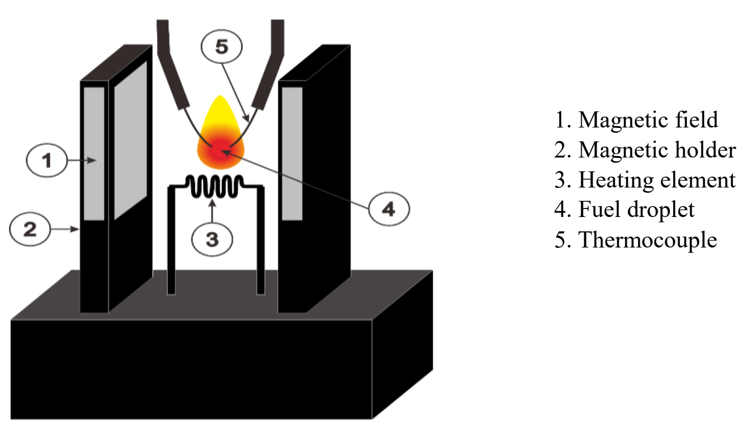

Figure 1. Details of magnetic field and droplet position

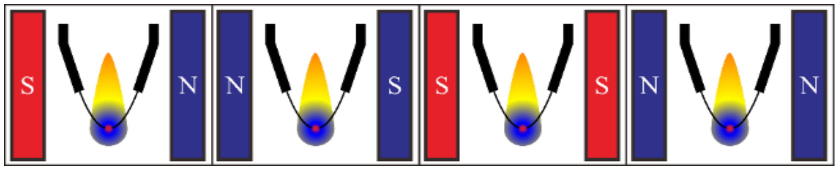

Figure 2. Magnetic field orientation

The magnetic field variable in this study was a 1.1 Tesla neodymium magnet with a pole spacing of 2 cm. As shown in Figure 2, the magnetic field was configured in four different directions: North–South (N–S), South–North (S–N), North–North (N–N), and South–South (S–S). The purpose of this configuration was to evaluate the effect of magnetic field direction on flame morphology, combustion temperature, combustion rate, flame height, and ignition delay time. To maintain the same magnetic strength for each variable, the magnetic field strength is checked using a TD8620 gauss meter at each change in magnetic configuration.

To avoid external disturbances such as wind and changing weather, the thermocouple, magnet, and heater circuit are placed in a 30 cm^3 enclosed space (5). This space is designed for quiescent conditions with an ambient temperature as shown in Figure 3. To trigger the combustion process, an electric current is supplied through a DC power supply with a predetermined voltage (6), so that heating can occur stably. This heater functions as an initial energy source that heats the droplets until they reach the flash point. Meanwhile, to measure the flame temperature, a thermocouple sensor is used which is connected to the AD8495 digital converter module (3) and the Arduino Uno microcontroller (2). The AD8495 module functions as a converter of analog signals from the thermocouple into high-resolution digital data, which is then read by the Arduino and sent to the computer (1) for real-time data recording. To ensure data accuracy, each test was carried out 3 times on each research variable. In addition, the visual data collection process is carried out using a high-speed camera (4) directed perpendicular to the droplet to record the flame and analyze its shape and stability.

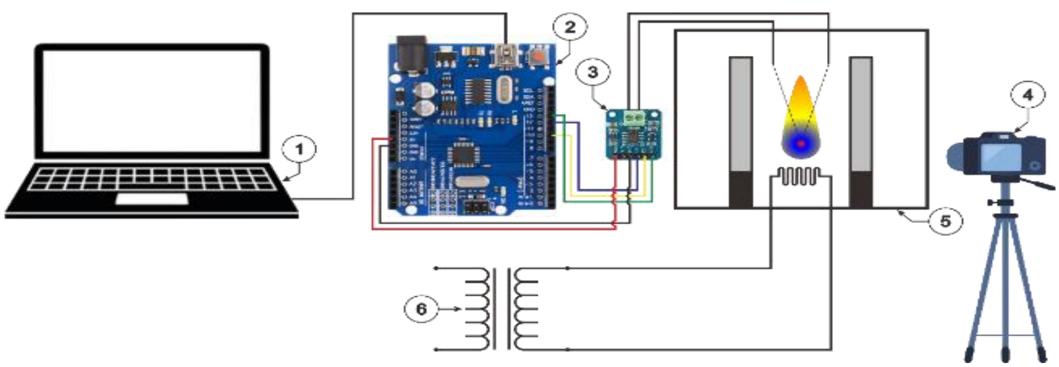

Figure 3. Schematic droplet combustion experiment : 1. Computer, 2. Arduino Uno, 3. Module thermocouple AD8495, 4. High-speed camera, 5. Combustion Chamber, 6. Power supply DC.

3. RESULTS AND DISCUSSION

3.1. Flame Evolution

Visual analysis of flame evolution is a fundamental step in understanding qualitative changes in combustion dynamics. Figure 4 presents a comparison of flame evolution for the five experimental conditions. This figure clearly illustrates that the presence and configuration of a magnetic field fundamentally alter the structure and behavior of the flame compared to the condition without a magnetic field (WOM).

In combustion without the influence of an external magnetic field, the combustion process is strongly influenced by the characteristics of the VCO fuel and natural fluid dynamics. As a biofuel, VCO, which is dominated by lauric acid (C12:0), has high oxidative stability, which implies a greater activation energy to initiate the reaction. Once combustion occurs, the process is controlled by buoyancy forces. This slow natural convection flow causes the mixing of fuel vapor and oxidizer to be inefficient. As a result, the combustion duration is the longest (2,340 s) and the flame appears tall and yellowish, indicating incomplete combustion and soot production. Physically, the flame in the WOM configuration shows instability characterized by an easily observed flickering phenomenon. This instability is most clearly seen in the final stage of combustion. After the flame reaches its maximum height at 1,872 s, there is a drastic reduction in flame height at 2,028 s, then appears to increase slightly again at 2,184 s before finally extinguishing. This oscillatory behavior reflects the inherent hydrodynamic instability of the flow due to the dominance of buoyancy. The interaction between the rising hot gas column and the surrounding cold air triggers the formation of vortices that then periodically detach, resulting in fluctuations in the reactant supply and variations in the heat release rate. This behavior contrasts sharply with the other four conditions (N-S, S-N, S-S, and N-N), where the flame gradually and smoothly decreases until it goes out, indicating complete suppression of instability.

In contrast, in the N-S (Figure 4d) and S-N (Figure 4e) magnetic field configurations, the flame visualizations exhibit strikingly contrasting characteristics. The flame appears much brighter, more focused, and has the shortest lifetime (~2,028 s), qualitatively indicating the most significant increase in efficiency and combustion rate. This improved combustion performance can be explained by two main mechanisms. First, the N-S and S-N configurations create a concentrated magnetic field with the strongest gradient across the pole gap, effectively exerting a Lorentz force on the charged particles in the flame and inducing a strong ionic wind toward the flame base. Second, and more dominant, is the ability of this magnetic field gradient to draw paramagnetic oxygen (O_2) into the reaction zone. This phenomenon, known as magnetic convection, as described by Wakayama *et al*., (1996), drastically increases the oxidizer supply. This increased oxygen flow, in turn, drastically accelerates the chemical reaction process, thereby amplifying the intensity and accelerating the combustion dynamics.

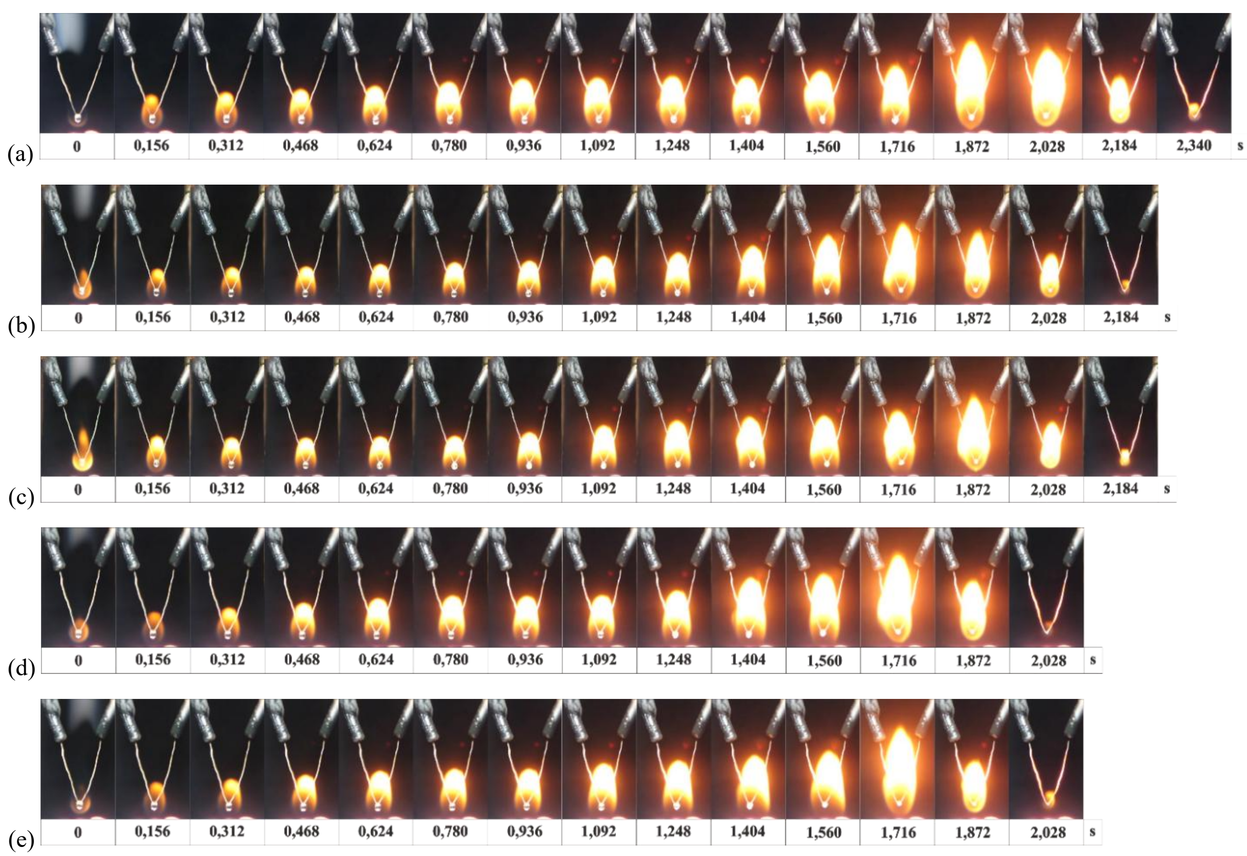

Figure 4. Visual flame evolution versus time in various magnetic field configurations and without magnet (a) Without Magnet (WOM), (b) South-South (S-S), (c) North-North (N-N), (d) North-South (N-S), (e) South-North (S-N)

In the repulsive magnetic field configuration N-N (Figure 4c) and S-S (Figure 4b), an increase in combustion efficiency was observed, indicated by a shorter flame duration (~2,184 s) compared to the non-magnetic condition (WOM), although it was still not as effective as in the attractive-magnetic configuration. The wider and less focused flame morphology is a consequence of the field topology that tends to spread the paramagnetic oxygen flow towards the outer side of the droplet.

This occurs due to the outward-bowing topology of the magnetic field in the repulsive configuration. This field shape creates a weaker magnetic field zone or even a null point directly above the droplet, so that the attractive force on the paramagnetic oxygen is not concentrated. These results further confirm that the magnetic field, through its role in manipulating the distribution of paramagnetic oxygen and the influence of the Lorentz force on charged particles, has a direct impact on flame structure, stability, and efficiency. These findings, particularly regarding the complete suppression of hydrodynamic instability by the magnetic field, confirm the results found by (Perdana *et al*., 2022), although their study was conducted on the combustion of coconut oil premix. This indicates that the mechanism of flame stabilization by magnetic fields is a fundamental phenomenon applicable to various types of fuels.

3.2. Flame Temperature

The temperature profiles during the observations for the five experimental conditions, measured using K-type thermocouples, are shown in Figure 5. This data analysis not only validates the findings from the visual analysis results, but also provides deeper quantitative insights into the thermal effects of each magnetic field configuration.

This analysis confirms that all magnetic field configurations consistently produce higher peak temperatures compared to the no magnetic field (WOM) condition. Specifically, the peak temperature sequence obtained is: S-N (858 °C) > NS (810 °C) > SS (790 °C) > NN (775 °C) > WOM (761 °C). In addition, the heating dynamics also undergo significant changes. The temperature curves in all magnetic conditions show a faster rate of temperature increase and a shorter time to reach the peak, in contrast to the WOM case where the increase is slower and only reaches the peak at 6.7 s. The observed temperature increase is generally a direct thermodynamic consequence of the increased oxidizer supply to the reaction zone, a mechanism that has been explained in the discussion of flame visualization. The forced convection flow generated by the paramagnetic force on molecular oxygen (O_2) significantly enriches the oxidizer concentration around the droplet. This condition drives the fuel-air ratio closer to the stoichiometric composition, resulting in a more perfect and efficient combustion process, as explained by the following reaction. This higher rate of energy release per unit time is what is measured as an increase in the overall flame temperature.

$$C_{12}H_{24}O_2 + 17O_2 \rightarrow 12CO_2 + 12H_2O + \text{heat} \tag{1}$$

The difference in peak temperatures between magnetic configurations can be explained by variations in the oxygen flow topology formed by the influence of the magnetic field. The highest temperatures achieved in the N-S and S-N configurations are a consequence of a more focused and concentrated oxygen supply mechanism. The strong field gradient between the pole gaps produces a jet-like oxygen flow directed directly into the flame core, thus creating a reaction zone with a very high energy density. In contrast, the relatively lower peak temperatures in the S-S and N-N configurations result from a more diffuse oxygen distribution to the outer part of the flame. While still significantly improving combustion efficiency, this wider reaction zone geometry has a larger surface area, thus increasing the potential for heat loss to the environment and lowering the peak temperature compared to the N-S/S-N case.

The performance differences between the S-N (858 °C) and N-S (810 °C) configurations, which are also observed for the S-S and N-N configurations, cannot be explained solely by paramagnetic effects, which are essentially identical. These subtle but consistent variations are a quantitative indication of second-order physical mechanisms, namely the Lorentz Force and ionic wind. As mentioned previously, the direction of the ionic wind vortices within the flame is opposite between the S-N and N-S configurations (Perdana *et al*., 2020). These different vortex orientations interact differently with the main fuel and oxygen streams, resulting in small variations in mixing efficiency at the microscale. Temperature data indicate that in this study the S-N configuration creates more optimal mixing conditions than the NS configuration, ultimately resulting in greater energy release and higher peak temperatures.

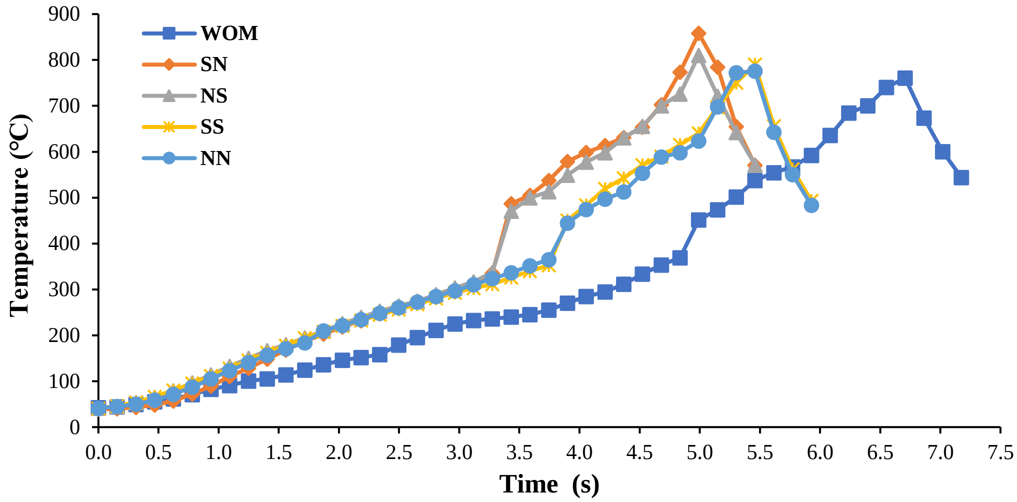

Figure 5. Flame temperature versus time at various magnetic field configurations and without magnet

3.3. Flame Height

To complement the morphological analysis, the evolution of the flame height during the combustion process was measured quantitatively and is shown in Figure 6. These data provide important insights into the flame dynamics that are not fully visible from visual observations. At the initial ignition (t = 0), the S-S and N-N field configurations produced the highest initial flame heights (7.74 mm and 5.52 mm), while the condition without a magnetic field (WOM) produced the lowest (2.57 mm). This phenomenon is the influence of the magnetic field on the formation of a reactive mixture cloud during the pre-combustion phase. In S-S/N-N, the paramagnetic oxygen flow that spreads around the droplet expands the reaction with the fuel vapor, resulting in a higher initial ignition. Conversely, in N-S/S-N, the more focused oxygen flow keeps the vapor cloud more concentrated, resulting in a lower initial flame height. In WOM, the absence of a magnetic field makes the fuel vapor diffusion slow, resulting in a smaller cloud and the lowest initial flame. Thus, the initial flame height reflects the mass transfer conditions in the pre-combustion phase, not the steady-state combustion dynamics. Interestingly, although SS and N-N produced the highest initial flame, the maximum flame height was achieved by WOM (16.58 mm). Meanwhile, N-S (16.42 mm) and S-N (16.29 mm) produced peaks nearly equivalent to WOM, while SS (14.70 mm) and N-N (14.40 mm) produced the lowest peaks.

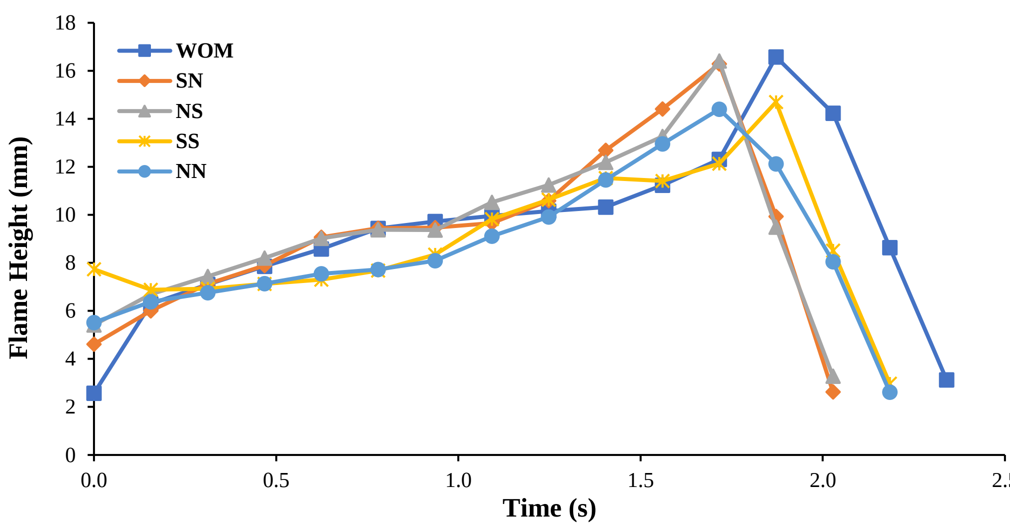

Figure 6. Flame height versus time at various magnetic field configurations and without magnet

This difference in flame height can be understood through the temporal dynamics of energy release. In the push-pull configurations (N-S and S-N), the supply of paramagnetic oxygen is consistent and intensive, resulting in very vigorous combustion within a short period. The rapid and massive energy release generates a vertical thrust that prolongs the flame momentarily. However, the high reaction rate also accelerates fuel consumption, resulting in a more rapid flame extinction. Thus, although the N-S/S-N configuration is capable of achieving maximum flame height, the resulting flame duration is relatively short.

In contrast, in the S-S and N-N configurations, the more diffuse oxygen distribution due to the outward curved field topology results in a more moderate heat release rate and is distributed over a wider basal reaction zone. The released energy is not concentrated on the vertical axis, but rather distributed across a wider basal reaction zone. This energy distribution suppresses the formation of a strong vertical flame column, resulting in a lower flame. This characteristic aligns with its bell-shaped visual morphology. In the WOM case, the dominance of slow buoyancy forces allows the flame to grow vertically longer before reaching the apex, resulting in a maximum flame height and a more towering visual impression.

Flame height analysis shows strong consistency with previous temperature data. The highest temperature peak in the N-S/S-N configuration coincides with the steepest flame height increase, both indicating the greatest energy release. Furthermore, the rapid decline in the N-S/S-N flame height after reaching the peak qualitatively indicates a very high burning rate. These parameters will be further analyzed quantitatively in the next section.

3.4. Burning Rate

The combustion rate is one of the most important quantitative parameters in the study of droplet combustion, as it directly reflects the efficiency and speed of fuel consumption. The combustion rate was determined by observing the evolution of the droplet diameter during the combustion process, then applying it to the d-squared law, which has long been recognized as a classical model for describing the phenomena of droplet evaporation and combustion.

$$\left(\frac{d}{D_0}\right)^2 = 1 - \frac{K.t}{D_0^2} \quad (2)$$

where d is the droplet diameter at time t, D_0 is the initial droplet diameter (t = 0), t is combustion time, and K is evaporation constant. The value of K is obtained from the negative slope (gradient) of the plot of $\left(\frac{d}{D_0}\right)^2$ versus time. The steeper the slope of the line formed, the greater the K value, which means the combustion rate is faster. In other words, this parameter not only provides a quantitative description of the speed of droplet exhaustion but also serves as a fundamental measure for comparing combustion efficiency under various experimental conditions.

The analysis results of the plot in Figure 7 clearly show that all magnetic field configurations provide a significant increase in the combustion rate of VCO droplets compared to the condition without a magnetic field (WOM). Based on the decreasing gradient of the curve $\left(\frac{d}{D_0}\right)^2$, the order of combustion rates from highest to lowest is: (N-S ≈ S-N) > S-S > N-N > WOM. This finding also serves as a final quantitative validation of the qualitative observations (flame duration) and thermal analysis (temperature) that have been described previously.

This discussion of results directly summarizes and integrates all previous findings into a cohesive narrative. The highest combustion rates in the N-S and S-N configurations are a direct consequence of the focused and efficient paramagnetic oxygen supply mechanism, which simultaneously results in the highest flame temperatures. These high temperatures significantly intensify the rate of heat feedback, both by conduction and radiation, from the flame to the droplet surface. This increased heat feedback accelerates the fuel evaporation process, thereby increasing the rate of release of combustible fuel vapor, which in turn accelerates the overall droplet diameter shrinkage rate. This positive relationship between flame temperature and combustion rate constant is consistent with findings in the droplet baking literature (Law, 2006). Therefore, the N-S and S-N configurations produce the highest combustion rate constants (K) compared to other conditions.

The measured intermediate burning rates in the S-S and N-N field configurations also show full consistency with the morphological and thermal analyses discussed previously. In these conditions, the peripherally driven oxygen supply

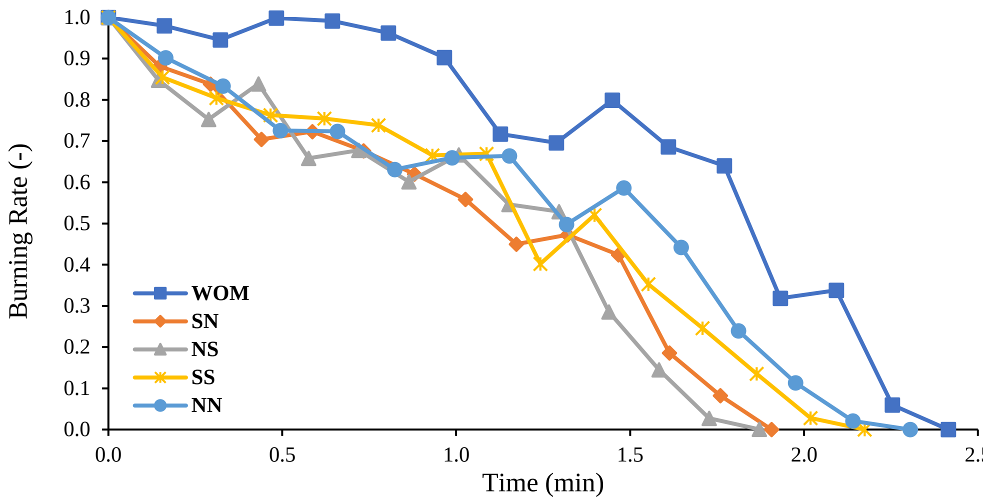

Figure 7. Burning rate versus time in various magnetic field configurations and without magnet

does increase efficiency compared to WOM, but not as intensively as the focused oxygen supply in the N-S/S-N configuration. This wider oxygen distribution results in a lower peak temperature, thus reducing the rate of heat feedback to the droplet surface. Consequently, the burning rates in the S-S and N-N cases fall between those in the WOM and N-S/S-N conditions. Conversely, the lowest burning rate in the WOM case is solely due to the very slow natural convection mechanism. This condition results in the lowest flame temperature, the weakest heat feedback, and the slowest fuel consumption rate.

The measured intermediate burning rates in the S-S and N-N field configurations also show full consistency with the morphological and thermal analyses discussed previously. In these conditions, the peripherally driven oxygen supply does increase efficiency compared to WOM, but not as intensively as the focused oxygen supply in the N-S/S-N configuration. This wider oxygen distribution results in a lower peak temperature, thus reducing the rate of heat feedback to the droplet surface. Consequently, the burning rates in the S-S and N-N cases fall between those in the WOM and N-S/S-N conditions. Conversely, the lowest burning rate in the WOM case is solely due to the very slow natural convection mechanism. This condition results in the lowest flame temperature, the weakest heat feedback, and the slowest fuel consumption rate.

Overall, the results of this combustion rate analysis provide quantitative validation that concludes the entire discussion. It is evident that the flame morphology modulated by the magnetic field is a visual representation of the oxidizer supply efficiency, which then determines the flame thermal environment, and ultimately controls the fuel consumption rate. The consistent cause-and-effect relationship between these three parameters results in a comprehensive understanding of the combustion mechanism of VCO droplets under the influence of a magnetic field.

3.5. Ignition Delay Time

From the measurement results in Figure 8, it can be seen that the configuration (WOM) produces the longest ignition delay time (IDT), namely 4.992 s, while the S-N and N-S configurations are able to accelerate ignition to 3.432 s. Meanwhile, the S-S and N-N configurations showed an intermediate IDT, which was 3.9 s. This difference confirms the significant role of the magnetic field in modifying the initial dynamics of the chemical reaction in droplet combustion. In the WOM condition, the ignition process is slower because the oxygen supply around the droplet relies solely on natural diffusion. In addition, the high viscosity of VCO causes the transport of fuel vapor to the oxidation zone to be slow, so the buildup of the reactive mixture required for flame initiation is delayed. These factors explain why the WOM has the longest IDT compared to the configuration with a magnetic field.

In contrast, in the S-N and N-S configurations, the magnetic field operates in an attractive mode, creating a strong flux gradient around the droplet. This condition accelerates the migration of paramagnetic oxygen molecules while simultaneously influencing the movement of free radicals during the pre-ignition phase. This accelerated transport of oxygen and fuel to the reaction zone triggers the faster formation of active radicals (OH• and H•), so that the initiation reaction proceeds with high efficiency. As a result, the IDT is significantly reduced to 3.432 s, indicating an accelerated ignition process due to the dominance of the oxidizer supply mechanism and the intensification of the initial reaction kinetics.

For the S-S and N-N configurations, the magnetic field operates in a repulsive mode, resulting in a diffuse flux distribution pattern and a stagnation area around the droplet. This condition reduces the efficiency of oxygen and fuel mixing because the paramagnetic oxygen flow is more dispersed to the periphery, not as effective as the focused supply in the S-N/N-S case. As a result, although the IDT is accelerated compared to the WOM condition, its value is only at an intermediate level (3.9 s). Overall, these results confirm that the S-N/N-S configuration provides the most optimal conditions for accelerating the ignition of VCO droplets, in line with the principle of magnetohydrodynamics (MHD) which explains that magnetic fields are able to accelerate the dynamics of charged particles and improve initial mixing in liquid combustion systems.

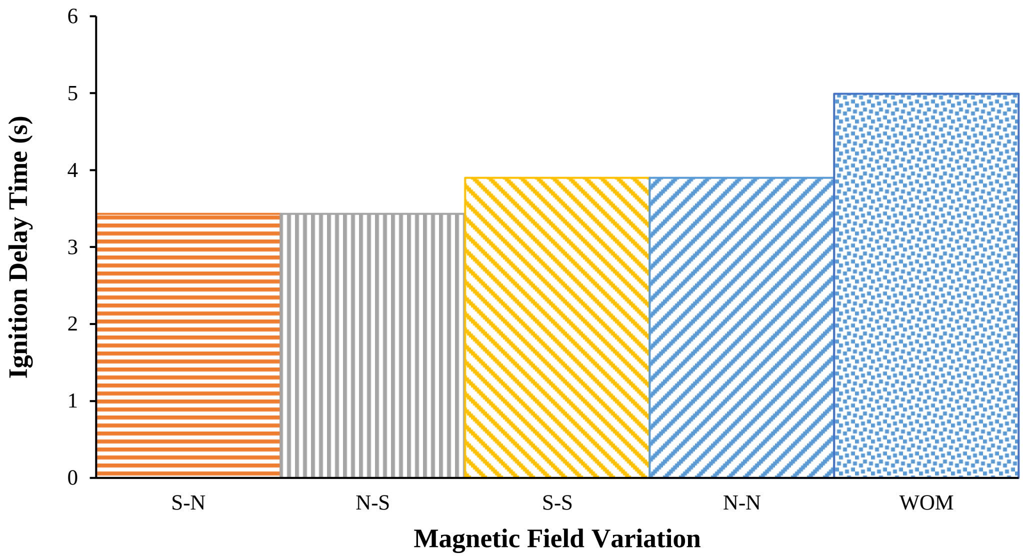

Figure 7. Ignition delay time for various magnetic field configurations and without magnet

4. CONCLUSIONS

This study demonstrates that the application of an external magnetic field significantly improves the combustion performance of a single-droplet VCO. This improvement is evident through the suppression of flickering instability, an increase in peak temperature up to 858 °C, an acceleration of the combustion rate, and a shortening of the ignition delay time. Furthermore, the magnetic field topology is proven to be a crucial controlling parameter, where the attractive-attractive (N–S/S–N) configuration consistently shows the most optimal performance compared to the repulsive-repellent configuration.

AUTHOR CONTRIBUTION STATEMENT

Author	C	M	So	Va	Fo	I	R	D	O	E	Vi	Su	P	Fu
WAW	✓	✓	✓	✓				✓	✓					✓
YHL						✓	✓			✓	✓		✓	

C: Conceptualization	Fo: Formal Analysis	O: Writing - Original Draft	Fu: Funding Acquisition
M: Methodology	I: Investigation	E: Writing - Review & Editing	P: Project Administration
So: Software	D: Data Curation	Vi: Visualization	
Va: Validation	R: Resources	Su: Supervision	

REFERENCES

Abdul Malik, M.S., Mohamad Shaiful, A.I., Mohd. Ismail, M.S., Mohd Jaafar, M.N., & Mohamad Sahar, A. (2017). Combustion and emission characteristics of coconut-based biodiesel in a liquid fuel burner. *Energies, **10***(4), 458. https://doi.org/10.3390/en10040458

Agarwal, S., Kumar, M., & Shakher, C. (2015). Experimental investigation of the effect of magnetic field on temperature and temperature profile of diffusion flame using circular grating Talbot interferometer. *Optics and Lasers in Engineering, **68***, 214-221. https://doi.org/10.1016/j.optlaseng.2015.01.004

Dedison, G., & Ismet, M.H. (2022). Effect of extracting method of coconut oils on tribological properties as bio-based lubricant. *Journal of Applied Engineering Science, **20***(3), 831–840. https://doi.org/10.5937/jaes0-32294

El-Fakharany, M.K., Abdelrazek, A.S., Baz, F.B., & Gad, M.S. (2025). Impact of nano-TiO_2 combination with biodiesel on diesel engine performance and emissions under fuel magnetism conditioning. *Arabian Journal for Science and Engineering, **50***, 14149–14164. https://doi.org/10.1007/s13369-024-09643-w

Ferreira de Souza, E., dos Santos Silva, R., Santos, M.N., de Andrade Silva, C.A., & Fiorucci, A.R. (2020). Evaluation of oxidative stability, fatty acid profile and quality physico-chemical parameters of Brazil nut, coconut and palm oils. *Ciência e Natura, 42*, Article 40894. https://doi.org/10.5902/2179460X40894

Hoxie, A., Schoo, R., & Braden, J. (2014). Microexplosive combustion behavior of blended soybean oil and butanol droplets. *Fuel, **120***, 22–29. https://doi.org/10.1016/j.fuel.2013.11.036

Hu, S., Hong, Z., Gao, J., Yang, X., Wang, L., Li, R., & Li, Y. (2022). Effect of magnetic field on alkane gas explosions. *Combustion and Flame, **246***, 112427. https://doi.org/10.1016/j.combustflame.2022.112427

Ibadurrohman, I.A., Hamidi, N., & Yuliati, L. (2023). Droplet combustion characteristics analysis based on the difference in carbon chain length of saturated fatty acid methyl ester as biodiesel constituents. Research Aspects in Chemical and Materials Sciences, **1**. https://doi.org/10.9734/bpi/racms/v1/2462B

IEA. (2024). *CO_2 emissions in 2023*. International Energy Agency. https://www.iea.org/reports/co2-emissions-in-2023.

Jocher, A., Pitsch, H., Gomez, T., Bonnety, J., & Legros, G. (2017). Combustion instability mitigation by magnetic fields. *Physical Review E, **95***, 063113. https://doi.org/10.1103/PhysRevE.95.063113

Khlaif, A.M., Abdul Wahhab, H.A., & Ehyaei, M.A. (2023). Impact of magnetic field on the stability of laminar flame in a counter burner. *International Journal of Energy Production and Management, **8***(4), 229–234. https://doi.org/10.18280/ijepm.080404

Kurji, H.J., & Imran, M.S. (2018). Magnetic field effect on compression ignition engine performance. *ARPN Journal of Engineering and Applied Sciences, **13***(12), 3943–3949.

Law, C.K. (2006). *Combustion Physics*. Cambridge University Press. https://doi.org/10.1017/CBO9780511754517

Leung, D.Y.C., Wu, X., & Leung, M.K.H. (2010). A review on biodiesel production using catalyzed transesterification. *Applied Energy, **87***(4), 1083–1095. https://doi.org/10.1016/j.apenergy.2009.10.006

Ma, F., & Hanna, M.A. (1999). Biodiesel production: A review. *Bioresource Technology, **70***(1), 1–15. https://doi.org/10.1016/S0960-8524(99)00025-5.

Marlina, E., Wijayanti, W., Yuliati, L., & Wardana, I.N.G. (2020). The role of pole and molecular geometry of fatty acids in vegetable oils droplet on ignition and boiling characteristics. *Renewable Energy, **145***, 596–603. https://doi.org/10.1016/j.renene.2019.06.064

Moser, B.R. (2009). Biodiesel production, properties, and feedstocks. *In Vitro Cellular & Developmental Biology – Plant, **45***, 229–266. https://doi.org/10.1007/s11627-009-9204-z

Parveg, A.S.M.S., & Ratner, A. (2025). Droplet-scale combustion analysis of third-generation biodiesel–diesel blends. *Energies, **18***(7), 1692. https://doi.org/10.3390/en18071692

Perdana, D., Adiwidodo, S., Subagyo, & Winarko, W.A. (2022). The role of perforated plate and orientation of the magnetic fields on coconut oil premixed combustion. *INMATEH – Agricultural Engineering, **67***(2), 77–84. https://doi.org/10.35633/inmateh-67-07

Perdana, D., Wardana, I.N.G., Yuliati, L., & Hamidi, N. (2018). The role of fatty acid structure in various pure vegetable oils on flame characteristics and stability behavior for industrial furnace. *Eastern-European Journal of Enterprise Technologies,* ***5***(8(95)), 65–75. https://doi.org/10.15587/1729-4061.2018.144

Perdana, D., Yuliati, L., Hamidi, N., & Wardana, I.N.G. (2020). The role of magnetic field orientation in vegetable oil premixed combustion. *Journal of Combustion,* ***2020***(1), 2145353. https://doi.org/10.1155/2020/2145353

Pham, P.X., Nguyen, K.T., Pham, T.V., & Nguyen, V.H. (2020). Biodiesels manufactured from different feedstock: From fuel properties to fuel atomization and evaporation. *ACS Omega,* ***5***(33), 20842–20853. https://doi.org/10.1021/acsomega.0c02376

Pliss, E.M., & Soloviev, M.E. (2022). Magnetic field effect on the oxidation of unsaturated compounds by molecular oxygen. *Magnetochemistry,* ***8***(4), 44. https://doi.org/10.3390/magnetochemistry8040044

Pramodkumar, G., Naidu, M.K., Sandeep, J.V., Vasupalli, R., & Lade, P. (2017). Effect of magnetic field on the emissions of single cylinder four stroke petrol engine. *Advances in Automobile Engineering,* ***6***(4). https://doi.org/10.4172/2167-7670.1000175

San José Alonso, J.F., Romero-Ávila, C., San José Hernández, L.M., & Awf, A.K. (2012). Characterising biofuels and selecting the most appropriate burner for their combustion. *Fuel Processing Technology,* ***103***, 39–44. https://doi.org/10.1016/j.fuproc.2011.07.023

Sharma, V., Hossain, A.K., & Duraisamy, G. (2021). Experimental investigation of neat biodiesels' saturation level on combustion and emission characteristics in a CI engine. *Energies,* ***14***(16), 5203. https://doi.org/10.3390/en14165203

Sidheshware, R.K., Ganesan, S., & Bhojwani, V. (2022). An effective reduction of exhaust emissions from combustive gases by providing a magnetic field through the fuel supply line: SI engine, CI engine, and LPG gas stove. *Energy storage systems*, 365–384. https://doi.org/10.1007/978-981-19-4502-1_17

Singh, S.P., & Singh, D. (2010). Biodiesel production through the use of different sources and characterization of oils and their esters as the substitute of diesel: A review. *Renewable and Sustainable Energy Reviews,* ***14***(1), 200–216. https://doi.org/10.1016/j.rser.2009.07.017

Srivastava, A., & Prasad, R. (2000). Triglycerides-based diesel fuels. *Renewable and Sustainable Energy Reviews,* ***4***(2), 111–133. https://doi.org/10.1016/S1364-0321(99)00013-1

Statista. (2025). *World Coconut Production by leading producers (2023)*. https://www-statista-com.translate.goog/statistics/1040499/world-coconut-production-by-leading-producers/

Wakayama, N.I., Ito, H., Kuroda, Y., Fujita, O., & Ito, K. (1996). Magnetic support of combustion in diffusion flames under microgravity. *Combustion and Flame,* ***107***(1–2), 187–192. https://doi.org/10.1016/0010-2180(96)00053-3

Wang, M., Wu, M., & Huo, H. (2007). Life-cycle energy and greenhouse gas emission impacts of different corn ethanol plant types. *Environmental Research Letters*, ***2***(2), 024001. https://doi.org/10.1088/1748-9326/2/2/024001

Winarko, W.A., Ilminnafik, N., Kustanto, M.N., & Perdana, D. (2022). Karaktersitik pembakaran droplet minyak nabati Indonesia. *Dinamika Teknik Mesin: Jurnal Keilmuan dan Terapan Teknik Mesin*, ***12***(2). https://doi.org/10.29303/dtm.v12i2.540

Y. Xie, Z. Wei, T. Zhou, H. Zhen, Z. Liu, and Z. Huang. (2021). Combustion Characteristics of Small Laminar Flames in an Upward Decreasing Magnetic Field. *Energies,* 1–18. https://doi.org/10.3390/en14071969

Zhu, M., Setyawan, H.Y., Zhang, Z., & Zhang, D. (2020). Effect of n-butanol addition on the burning rate and soot characteristics during combustion of single droplets of diesel–biodiesel blends. *Fuel,* ***265***, 117020. https://doi.org/10.1016/j.fuel.2020.117020